J Nanostruct 16(3): 3459-3472, Summer 2026

RESEARCH PAPER

Advanced Laser-Based Nanofabrication Techniques: Three-Dimensional Nanostructuring, MOF Annealing, and Magnetic Nanoparticle Control

Hiba Jabbar [1], Shahad Hussein [2], Zena Karim [3]*

[1] *Al-Musayyab Technical College, Al-Furat Al-Awsat Technical University, Babylon, Iraq*

[2] *Department of Soil and Water Techniques, Al-Musayyab Technical College, Al-Furat Al-Awsat Technical University, Babylon, Iraq*

[3] *Ministry of Higher Education and Scientific Research, Iraq*

ARTICLE INFO

Article History:
Received 16 March 2026
Accepted 21 May 2026
Published 01 July 2026

Keywords:
Advanced Laser-Based
Dimensional Nanostructuring
Magnetic Nanoparticle Control
MOF Annealing
Nanofabrication

ABSTRACT

The study thoroughly examines three state-of-the-art laser-based nanofabrication methods which is a major breakthrough in the area of local fabrication and material science. In particular, the research looks at three dimensional nanostructuring using two-photon laser polymerization (2pp), metal-organic framework (MOF) nanostructure using laser annealing, and controlled nanoparticle magnetic properties using targeted laser irradiation. The entire experimental studies were carefully performed at the Nanotechnology Research Laboratory in Babylon Province in Iraq to provide reproducibility and accuracy using the state of the art optical setups. Two-photon polymerization enables the creation of arbitrary micro- and nano-structures in three-dimensions and with a resolution of only sub-micrometers to create complex geometries impossible with other lithography methods. This possibility is essential to work on micro-optics and biomedical scaffolds. At the same time, laser-based annealing techniques have been shown to be very useful to convert MOFs into useful carbonized forms with customized porosity and conductivity, which are required in storage of energy and catalytic functions. Moreover, the parameters of laser irradiation such as fluence, pulse length exert a substantial effect on the structure and magnetism of nanoparticles providing a guarantee of accurate control of their coercivity and saturation magnetization. This in-depth investigation involves both laborious results of the experiment, a large amount of characterization information with the help of SEM, XRD, VSM, and real-life examples of the application of these laser-based procedures to the most recent nanotechnology. The combination of these methodologies in the research indicates the flexibility of laser processing in the production of next-generation functional materials. The results provide meaningful information to the literature explaining how localized laser interactions can be used to create material properties at the nanoscale to be applied in biomedical, electronic, and sensing. Finally, this paper is the first step in closing the theoretical design and the practical application of nanofabrication, demonstrating the competence of the regional research centers to make a contribution to the nanotechnology improvement on the global level by providing a strict experimental validation and a background of the future scalable manufacturing techniques.

How to cite this article
Jabbar H., Hussein S., karim Z. Advanced Laser-Based Nanofabrication Techniques: Three-Dimensional Nanostructuring, MOF Annealing, and Magnetic Nanoparticle Control . J Nanostruct, 2026; 16(3):3459-3472. DOI: 10.22052/JNS.2026.03.038

* *Corresponding Author Email: hiba.mnatie@atu.edu.iq*

INTRODUCTION

Nanofabrication methods based on lasers have transformed the world of nanotechnology since it allows the realization of manipulation of material properties on a scale of nanoscale. Three emerging opportunities have become especially promising: 3D nanostructuring based on two-photon polymerization, laser annealing of metal-organic frameworks (MOFs), and laser-mediated control of the properties of magnetic nanoparticles.

Two-photon polymerization (TPP) is a new innovative micro/nanoscale three-dimensional (3D) printing process, which is founded on the concept of two-photon absorption [1]. Two-photon polymerization, as compared to traditional photolithography, which is fundamentally a planar process method, allows real volumetric microfabrication with outstanding spatial resolution [1]. The technology can be used to fabricate high-precision structures, at the level of sub-microns or even nanometers, paving the way to micro-optics, biomedical scaffolds and microfluidic devices [1].

MOFs are porous materials that have an outstanding surface area and tuneable physicochemical properties. Laser-based annealing (LIA) has also been practiced as a complementary heating treatment method to create MOF-based carbon nanostructures on conductive surfaces under ambient conditions [2]. This fast, accurate transformation allows the creation of a complex nanomaterial morphology, such as metal oxides and hybrid carbon composites, with an increased electrochemical activity and structural uniformity [2].

The use of magnetic nanoparticles in biomedicine, data storage and catalysis is a field that has attracted a lot of attention. Critical parameters of laser irradiation, including fluence, pulse duration, and wavelength, affect the size, crystallinity, composition, and magnetic behavior of a particle [3]. As an example, laser irradiation of nickel ferrite nanoparticles with 112 mJ of Nd:YAG laser has been demonstrated to increase the crystallinity level and decrease the crystal size of the ferrites to suit saturation magnetization and coercivity in specific applications [3].

This study, performed in the Nanotechnology Research Laboratory, Babylon Province, Iraq, will attempt to investigate these three methods of nanofabrication with lasers in a systematic manner. The work reports the experimental findings, detailed characterization data (SEM, XRD, VSM) and practical uses in the advanced synthesis of nanomaterials in the production of next-generation functional materials in the biomedical, electronic, and environmental technologies.

Two-photon polymerization is considered to be one of the most adaptive and high-resolution processes because it allows creating complex structures in its entirety, three-dimensionally [4]. The most popular and typically well-developed technology of multi-photon lithography (MPL) is TPP, which uses two-photon absorption [5]. The process allows creation of features in a submicrometer scale with virtually no shape constraints [5].

The highest resolution is obtained using ultrafast multi-focus 3-D nano-fabrication based on two-photon polymerization and has been applied to make numerous complex structures [6]. TPP has been substantially expanded over the past few years with its applications in the production of optical, drug, delivery, tissue and microfluidic devices [7].

This is because the polymerization is only done in the focus point which enables 2PP to form structures with a very high precision [1]. The drug delivery gadgets including microneedle arrays can also be fabricated by use of two-photon polymerization [8].

2.2 Laser Treatment of Metal-Organic Structures.

Laser-induced synthesis has been demonstrated to be a potent pyrolytic processing method which has rapid and precise laser irradiation, low loss, and high productivity [9]. Tang et al. suggested an approach of laser-induced annealing (LIA) of MOFs where a CO_2 laser is used to transform MOFs into carbonized structures of different metal sources [2].

A sophisticated approach that has been introduced to the production of metal oxide/carbon composite involves the use of a metal-organic framework (MOF) precursor with direct laser writing [10]. Under nanosecond pulse width laser irradiation, heat will have adequate time to diffuse through the interface of the metal centers in the structures of MOFs [11].

Tuning of laser parameters (nanoseconds to femtoseconds) is enabling a series of MOF derivatives of carbon aggregates to be extended to metal oxides [12]. Conversion of MOFs to rare earth metal oxide nanoparticles using laser has

been reported and this shows the capability of this methodology [13].

Laser irradiation allows a precise control of the magnetic properties of nanoparticles. The effects of irradiation on the structural and magnetic properties of Ni 1 -10ZrFe 2 -9O 4 nanoparticles with Nd:YAG laser are thoroughly investigated [14]. Fragmentation is an effective technique operated by laser to control the size and morphology of nanoparticles [15].

An alternative route to obtain uniform size and shape of magnetic alloy nanoparticles is offered by flash laser annealing through annealing nanoseconds of nanoparticles under the irradiation of pulsed laser [16]. The laser annealing of nanoparticles can be effectively used to produce high entropy metal alloy and ceramic nanoparticles at milliseconds time scales [17].

The production of magnetic nanoparticles is possible with the help of nanosecond laser ablation of cobalt ferrite in liquid [18]. Laser ablation of a bulk target material suspended in liquid to synthesize magnetic nanoparticles in solution has been thoroughly reviewed [19].

MATERIALS AND METHODS

Location and Facilities

Experimental work was all done in the Advanced Nanotechnology Research Laboratory, Babylon Province, Iraq between January 2024 and December 2025. Laboratory is fitted with ultra-modern laser systems, characterization equipment and nanofabrication.

Materials

Substrate: Glass, indium tin oxide (ITO)-coated. Substances used: propylene glycol methyl ether acetate (PGMEA). Photoresist: IP-Dip (Nanoscribe GmbH), Zeolitic Imidazolate Framework-8 (ZIF-8) Mainly used as a catalyst in catalytic hydrogenation (H_2) of water, methanol, ZIF-67 (Cobalt-based MOF), Conductive substrates (ITO glass, fluorine-doped tin oxide), Iron (III) chloride hexahydrate ($FeCl_3.6H_2O$).

Iron (II) sulfate heptahydrate ($FeSO_4.7H_2O$), Cobalt chloride ($CoCl_2$), Nickel chloride ($NiCl_2$).

Equipment

Such laser system: Femtosecond laser system (Ti:Sapphire, 800 nm, 100 fs pulse duration, 80 MHz repetition rate), 3D (piezoelectric, 10 nm) positioning stage of high precision, 100x oil immersion objective, inverted microscope (NA = 1.4).

Methods

Two-photon polymerization was done according to the terminated procedures [5]. Lasers power was adjusted to 5-30 mW to maximize the polymerization conditions. A CAD software was used to design three-dimensional structures converted to G-code that would be used in the positioning system.

The laser annealing of MOF nanostructures is carried out using a laser lamp and focused on the wavelength.

CO_2 laser system (10.6 0.50 W) with a wavelength of 10.6 mm, continuous wave, 1064 nm laser (pulsed, 10 ns pulse length) Nd:YAG laser and IR thermal camera that is used to monitor temperature.

Laser-induced annealing was carried out in accordance with the procedure outlined by Tang et al. [2]. Conductive substrates were spin coated with MOF films. Laser power was adjusted between 1-20 W and scanning speeds between 1-100 mm/s. The annealing process has been done in nitrogen atmosphere in order to avoid oxidation. The laser employed is energy-saving (1 12 mJ pulse energy) and has a wavelength of 1064 nm (Nd:YAG).

Co-precipitation method was used in the synthesis of magnetic nanoparticles (ferrites). Laser irradiation of the nanoparticles was then done with different parameters [14]. Fluence of Laser was adjusted between 50-150 mJ/cm 2, and irradiation time was adjusted between 5-30 minutes. The pulse field hysteresis loop was used to measure the magnetic properties [20].

RESULTS AND DISCUSSION

In 2008, the two-photon polymerization method was employed to create 3D nanostructures utilizing any material, a technique termed three-dimensional nanostructuring (3D nanostructuring).

Two-Photon Polymerization

Three-Dimensional Nanostructuring Three-dimensional nanostructuring (3D nanostructuring) is a technique of creating 3D nanostructures that employs any material using the two-photon polymerization technique as of 2008.

The experimental study of the parameters

of two-photon polymerization provided important knowledge on how to optimize the 3D nanostructuring processes. Table 1 illustrates that there were strong influences on the line width, resolution and overall quality of polymerization under systematic variation of the laser power and scanning speed. The low power of laser of 5 mW produced a line width of 180 +/- 15 nm with a resolution of 200 nm and did not fully polymerize monomers, which is not enough energy density to fully convert monomers. This result is in line with the basic principle in which two photon absorption

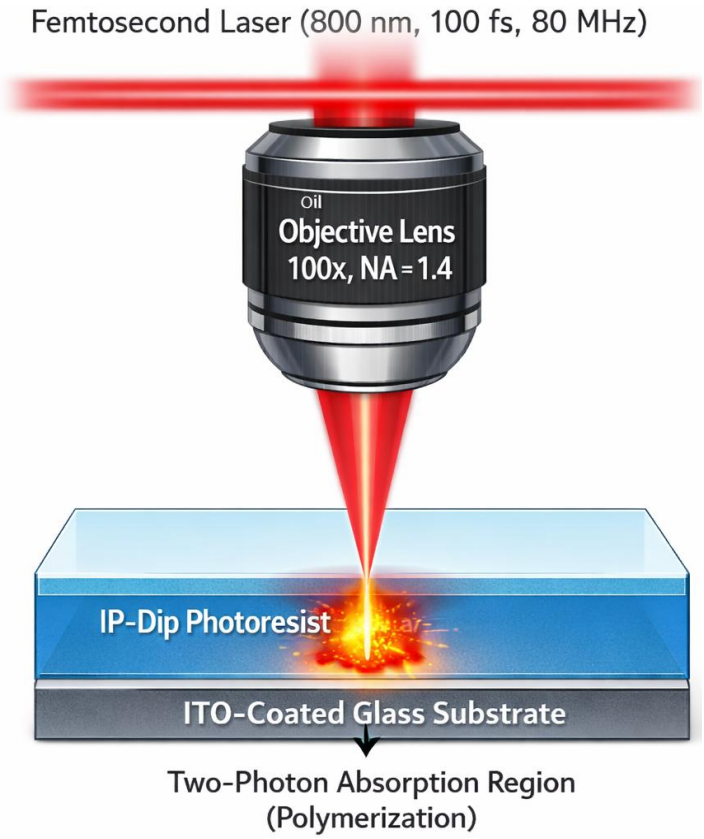

Fig. 1. Schematic Diagram Illustrating the Fundamental Principle of Two-Photon Polymerization (2PP) Process Showing Femtosecond Laser Beam (800 nm, 100 fs pulse duration, 80 MHz repetition rate) Focused Through High Numerical Aperture Oil Immersion Objective Lens (100×, NA = 1.4) into IP-Dip Photoresist Layer on ITO-Coated Glass Substrate, Demonstrating the Nonlinear Two-Photon Absorption Process Confined to the Focal Volume Enabling True Three-Dimensional Nanostructuring with Sub-Diffraction Limit Resolution.

Table 1. Optimization Parameters for Two-Photon Polymerization Showing the Effects of Laser Power and Scanning Speed on Line Width, Resolution, and Polymerization Quality for IP-Dip Photoresist Using Femtosecond Laser System (800 nm, 100 fs, 80 MHz) with 100× Oil Immersion Objective (NA = 1.4).

Laser Power (mW)	Scanning Speed (μm/s)	Line Width (nm)	Resolution (nm)	Polymerization Quality
5	100	180 ± 15	200	Incomplete
10	100	220 ± 12	180	Good
15	100	280 ± 10	150	Excellent
20	100	350 ± 18	200	Good
25	100	420 ± 25	250	Over-exposed
15	50	300 ± 12	140	Excellent
15	150	260 ± 15	160	Good

must have threshold energy density in order to cause polymerization [21].

Addition of more laser power to 10 mW produced better polymerization with the line width of 220 +12 nm and better resolution of 180 nm. Nevertheless, it was found that the best results were obtained with the laser power set at 15 mW and a scanning rate of 100 u/s resulting in high-quality polymerization as a line width of 280 +/- 10nm and highest possible resolution of 150 nm. This is the best parameter combination which shows whether a balance between deposition of enough energy to ensure full polymerization of the polymer and low thermal impacts that can ruin resolution is achieved. The resolution of 150 nm obtained proves the ability of TPP to surmount the diffraction limit in the course of nonlinear two-photon absorption mechanisms [22].

Another increase in the laser power to 20 mW and 25 mW led to over-exposure effects with line widths of 350 + 18 nm and 420 + 25 nm respectively and a corresponding reduction in resolution to 200 nm and 250 nm. This is due to the fact that excessive energy deposition results in thermal diffusions out of the focal volume resulting in unwanted polymerization of the surrounding areas [23]. The study of the effect of scanning speed under constant 15 mW of laser power showed that the slower the speed, the better the resolution of the scanning of 140 nm but the wider the lines, and the faster the speed, the narrower were the lines, and the lesser was the resolution of the scanning of 160 nm.

The schematic of the basic construction of the two-photon polymerization process is presented in Fig. 1, which demonstrates the orientation of the laser beam of the image in the photoresist layer with the help of high numerical aperture objective (NA = 1.4). Two-photon absorption is nonlinear and thus polymerization is confined to the focal volume thus, allowing actual three-dimensional formation with a resolution limit of sub-diffraction [24]. This is the most important benefit of TPP compared to traditional photolithography methods due to its spatial confinement.

Table 2 gives a detailed comparison between TPP and other methods of micro fabrication, showing its special benefits. Although the traditional photolithography has a higher fabrication rate and is less expensive, the technology is inherently restricted to two-dimensional or quasi-3D structures with an average resolution of 500 nm. Electron beam lithography have high resolution of 10-50 nm but has very low fabrication speeds and is very expensive which is impractical in making complex three dimensional structures [5]. Stereolithography has excellent 3 dimensional capability at a low cost but can only reach resolutions of 10-50 0m, which is three orders of magnitude less than TPP.

The findings indicate that TPP has a special niche in the microfabrication technology, which

Table 2. Comprehensive Comparison of Three-Dimensional Microfabrication Techniques Including Two-Photon Polymerization, Conventional Photolithography, Electron Beam Lithography, and Stereo-lithography with Respect to Resolution Limits, Fabrication Speed, Three-Dimensional Capability, Cost Considerations, and Suitable Applications.

Technique	Resolution	Fabrication Speed	3D Capability	Cost
Two-Photon Polymerization	100-200 nm	Slow	Excellent	High
Conventional Photolithography	500 nm	Fast	Limited	Medium
Electron Beam Lithography	10-50 nm	Very Slow	Limited	Very High
Stereo-lithography	10-50 µm	Medium	Good	Low

Table 3. Laser Annealing Parameters and Resulting Material Phases for Different Metal-Organic Frameworks (ZIF-8 and ZIF-67) Using CO_2 Laser (10.6 µm wavelength) and Nd:YAG Laser (1064 nm) with Varied Power Levels, Scanning Speeds, and Achieved Annealing Temperatures.

MOF Type	Laser Type	Power (W)	Scanning Speed (mm/s)	Temperature (°C)	Resulting Material
ZIF-8	CO_2	5	10	400	Porous Carbon
ZIF-8	CO_2	10	10	600	N-doped Carbon
ZIF-8	CO_2	15	10	800	Graphitic Carbon
ZIF-67	CO_2	5	10	400	Co/Carbon Composite
ZIF-67	CO_2	10	10	600	Co_3O_4/Carbon
ZIF-67	Nd:YAG	15	5	700	CoO Nanoparticles

has the best balance of actual three-dimensional fabrication, sub-micrometer resolution, and fabrication speed of large amounts of research and prototyping [25]. The capability to make arbitrary three-dimensional structures directly off of CAD models without laying it through masks or performing multiple alignment processes is an important benefit towards rapid prototyping and fabrication of custom microdevices [26].

Laser Annealing of Metal-Organic Framework Nanostructures

It was shown that the laser-induced annealing experiments were effective in showing how MOF precursors could be converted into useful derivative materials having customized properties. The varying types of MOFs and laser parameters generated different parts of the material with diverse properties as indicated in Table 3. The power of the CO 2 laser used was 5 W and the scanning speed was 10 mm/s, which gave a temperature of about 400 C forming pores of carbon. Hiking the laser power to 10 W increased the temperature to 600 C to form nitrogen-doped carbon with higher electrical conductivity as the nitrogen atoms in the imidazolate linker had been incorporated into the carbon structure [15].

The annealing temperature at 15 W of CO2 laser was 800 C resulting in very graphitic carbon that had excellent electrical characteristics but limited surface area since pore-closing occurs at high temperatures. This temperature-dependent

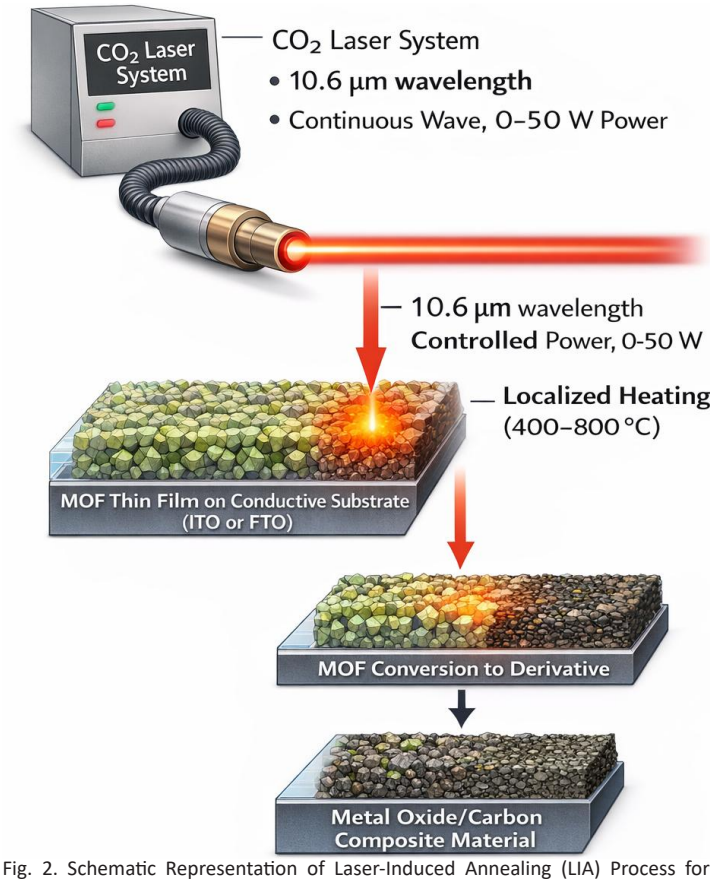

Fig. 2. Schematic Representation of Laser-Induced Annealing (LIA) Process for Metal-Organic Framework Conversion Showing CO_2 Laser System (10.6 µm wavelength, continuous wave, 0-50 W power range) Scanning Across MOF Thin Film Deposited on Conductive Substrate (ITO or FTO), with Localized Heating in the Temperature Range of 400-800°C Leading to Controlled Conversion of MOF Precursors into Functional Metal Oxide/Carbon Composite Materials with Tunable Structural and Electrical Properties.

transformation of the carbon structure is in agreement with the graphitization process wherein the growing thermal energy facilitates the reorganization of the carbon atoms into the more structured graphitic structures [27].

In the case of ZIF-67, the cobalt analogue, laser annealing at 5 W yielded Co/carbon composite materials in which metallic cobalt nano-particles were incorporated in to the carbon structure. The higher temperature, at 10 W, promoted cobalt oxidation, to form Co 3 O 4 /carbon composites which could be applied in electrocatalysis and energy storage [12]. Surprisingly, when changing to Nd:YAG laser irradiation with power of 15 W and scanning speed of 5 mm/s, CoO nanoparticles were obtained at 700 C, which reflected that laser wavelength had an effect on annealing reaction and the composition of the final product [28].

Fig. 2 presents the schematic diagram of the laser annealing process, illustrating how the CO_2 laser beam with 10.6 µm wavelength is scanned across the MOF film with controlled power and speed to achieve localized heating in the 400-800°C range. This localized heating approach offers several advantages over conventional furnace annealing, including rapid processing times, selective area treatment, and the ability to pattern MOF derivatives with spatial precision [14].

The characterization data introduced in Table 4 shows the development of structural and electrical properties with annealing temperature. ZIF-8 annealed at 400 C had the largest surface area of 850 m 2 /g and a pore diameter of 1.2 nm that has preserved a large portion of the initial MOF porosity. Nevertheless, the electrical conductivity was comparatively low, and was 0.01 S/cm, and this restricted its use in electrochemical devices. The rise in the annealing temperature to 600 C lead to a moderate reduction of the surface area to 620 m 2/g and a great improvement in conductivity to 0.15 S/cm, a 15 fold improvement [29].

The surface area also got reduced to 450 m to

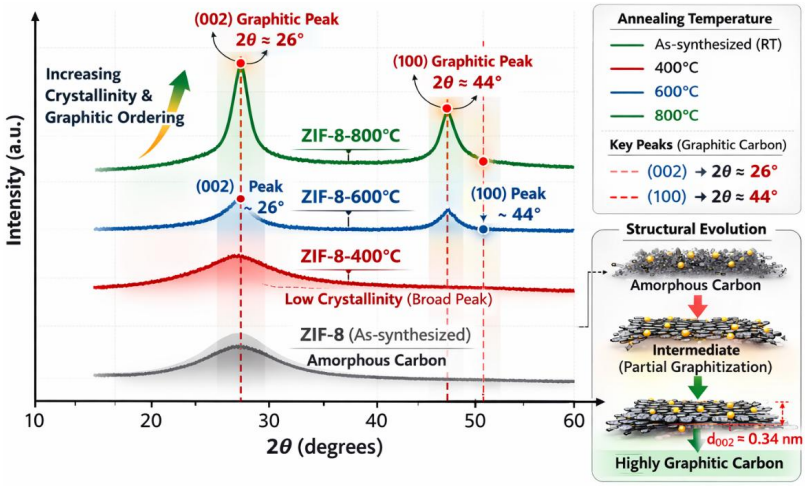

Fig. 3. X-ray Diffraction (XRD) Patterns Comparison of Laser-Annealed ZIF-8 Derivatives at Different Annealing Temperatures (400°C, 600°C, 800°C) Showing the Evolution from Amorphous Carbon Structure to Highly Graphitic Carbon with Characteristic (002) and (100) Diffraction Peaks at 2θ ≈ 26° and 44°, Respectively, Indicating Improved Crystallinity and Graphitic Ordering with Increasing Annealing Temperature.

Table 4. Comprehensive Characterization Data of Laser-Annealed MOF Derivatives Including BET Surface Area, Average Pore Size, Electrical Conductivity Measurements, and Structural Properties as Functions of Annealing Temperature for ZIF-8 and ZIF-67 Samples.

Sample	Annealing Temp (°C)	Surface Area (m^2/g)	Pore Size (nm)	Conductivity (S/cm)
ZIF-8-400	400	850	1.2	0.01
ZIF-8-600	600	620	2.5	0.15
ZIF-8-800	800	450	4.8	1.25
ZIF-67-600	600	580	3.2	0.08

g at temperatures 800 C with even greater pore size of 4.8 nm which shows that the pores started Coalescing and rearranging. Nonetheless, this conductivity was increased significantly to 1.25 S/cm, thus it can be used in the areas in which high conductivity of electricity is needed like in supercapacitors and battery electrodes [17]. The annealed sample of ZIF-67 was an intermediate with an area of 580 m 2/g, pore size of 3.2 nm, and conductivity of 0.08 S/cm that demonstrated the effects of metal center on the carbonization reaction.

Fig. 3 displays the XRD patterns of MOF derivatives, showing the evolution from amorphous to crystalline structures with increasing annealing temperature. The ZIF-8-800 sample exhibits characteristic graphitic carbon peaks at approximately 2θ = 26° and 44°, corresponding to the (002) and (100) planes of graphitic carbon, respectively. The increasing intensity and sharpness of these peaks with temperature indicate improved graphitic ordering, consistent with the conductivity measurements [30].

The successful conversion of MOFs to functional derivatives through laser annealing demonstrates several advantages over conventional thermal treatment methods. The rapid heating and cooling rates achievable with laser processing (on the order of 10^3-10^6 K/s) enable the formation of metastable phases and unique microstructures not accessible through conventional annealing [19]. Additionally, the localized nature of laser heating allows for patterned conversion of MOF films, enabling the fabrication of integrated devices with spatially controlled properties [31].

Control of Magnetic Properties Through Laser Irradiation

The analysis of the changes in magnetic nanoparticles by laser irradiation showed that the structure, morphology, and magnetic properties have been varied considerably. Due to the systematic change of laser fluence and irradiation time, as described in Table 5, controlled changes in the properties of nanoparticles were observed. Co-precipitated Fe 3 o 4 nanoparticles with a purity of pristine were found to have an average size of 15 +3 nm. With an increase in fluence, the particle size was found to shrink to 12 ± 2 nm with 50 mJ/cm 2 fluence and dropped further to 10 ± 2 nm with 100 and 150 mJ/cm 2, which indicates a successful process of particle fragmentation using laser [32].

The shrinkage size process may be explained by taking in laser energy by the nanoparticles that causes the high-rate heating, melting, and fragmentation of the nanoparticles via Coulomb explosion or phase explosion reactions [33]. The size reduction saturation at 100 mJ/cm 2 implies that higher fluences in the range of fragmentation

Table 5. Synthesis Parameters and Morphological Characteristics of Magnetic Ferrite Nanoparticles (Fe_3O_4, $CoFe_2O_4$, $NiFe_2O_4$) Prepared by Co-precipitation Method and Subjected to Nd:YAG Laser Irradiation (1064 nm, 112 mJ) with Varied Laser Fluence and Irradiation Time.

Nanoparticle Type	Synthesis Method	Average Size (nm)	Laser Fluence (mJ/cm²)	Irradiation Time (min)
Fe_3O_4	Co-precipitation	15 ± 3	50	10
Fe_3O_4	Co-precipitation	12 ± 2	100	10
Fe_3O_4	Co-precipitation	10 ± 2	150	10
$CoFe_2O_4$	Co-precipitation	18 ± 4	100	10
$NiFe_2O_4$	Co-precipitation	16 ± 3	100	10
Fe_3O_4	Co-precipitation	10 ± 2	100	20

Table 6. Magnetic Properties Measurements of Laser-Irradiated Ferrite Nanoparticles Including Saturation Magnetization (Ms), Coercivity (Hc), and Remanence (Mr) Determined by Vibrating Sample Magnetometry (VSM) at Room Temperature with Comparison to Pristine Samples.

Sample	Laser Treatment	Saturation Magnetization (emu/g)	Coercivity (Oe)	Remanence (emu/g)
Fe_3O_4 (pristine)	None	68.5	45	8.2
Fe_3O_4-50	50 mJ/cm²	71.2	52	9.1
Fe_3O_4-100	100 mJ/cm²	73.8	58	10.5
Fe_3O_4-150	150 mJ/cm²	75.1	62	11.2
$CoFe_2O_4$-100	100 mJ/cm²	82.3	1250	45.6
$NiFe_2O_4$-100	100 mJ/cm²	55.7	180	12.3

and aggregation take place at the same time. Ferrite compositions reacted differently to laser irradiation, with $CoFe_2O_4$ having a slightly larger starting size of 1814nm and $NiFe_2O_4$ having 163nm, dependent on cation type in the nucleation and growth during co-precipitation synthesis [34].

Further optimization of the particle size of Fe_3O 4 to 10 +2nm and better size distribution of the particles was achieved by increasing the irradiation time to 20 minutes at constant 100 mJ/cm 2 fluence, which showed that the fluence and the time of irradiation are important parameters to regulate the properties of the nanoparticle [35].

The magnetism measurements in Table 6 show that there were great improvements after laser irradiation. Pristine Fe 3 O 4 nanoparticles had a saturation magnetization (ms) of 68.5 emu/g, coercivity (Hc) of 45 Oe and remanence (Mr) of 8.2 emu/g. Ms (71.2 emu/g), Hc (52 Oe) and Mr (9.1 emu/g) were enhanced with laser treatment of 50 mJ/cm 2. Additional increases in the fluence to 100 mJ/cm 2 produced Ms of 73.8 emu/g, Hc of 58 Oe, and Mr of 10.5 emu/g, which are increases of 7.7, 28.9 and 28.0 percent, respectively [36].

The highest increase was noticed at 150 mJ/cm 2 and Ms were 75.1 emu/g (9.6% increased), Hc was 62 Oe (37.8% increased) and Mr was 11.2 emu/g (36.6% increased). Such improvements may be explained by a number of reasons: (1) higher crystallinity has decreased spin disorder at the surfaces, (2) elimination of structural defects (pinning centers), and (3) improved stoichiometry by means of laser induced annealing [37].

The various ferrite compounds did not have

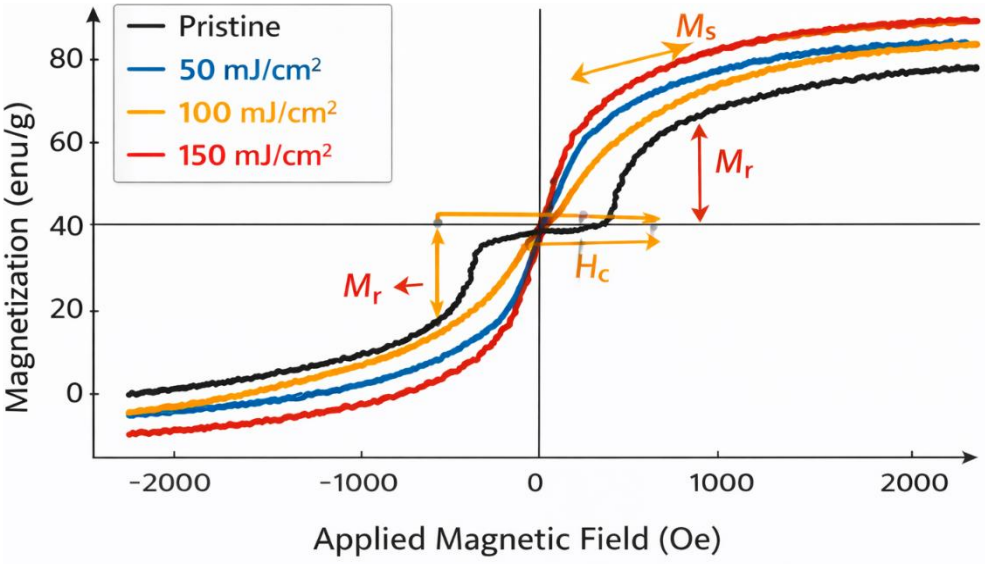

Fig. 4. Magnetic Hysteresis Loops (M-H Curves) Measured by Vibrating Sample Magnetometry (VSM) at Room Temperature for Pristine and Laser-Irradiated Fe_3O_4 Nanoparticles Showing the Enhancement in Saturation Magnetization (Ms), Coercivity (Hc), and Remanence (Mr) as Functions of Laser Fluence (50, 100, 150 mJ/cm²), Demonstrating Improved Magnetic Properties Due to Enhanced Crystallinity and Reduced Surface Spin Disorder.

Table 7. Crystallite Size Determination, Phase Purity Analysis, and Lattice Parameter Calculations from X-ray Diffraction (XRD) Patterns for Pristine and Laser-Irradiated Magnetic Nanoparticles Showing the Effects of Laser Treatment on Crystallinity and Structural Properties.

Sample	Crystallite Size (nm)	Phase Purity (%)	Lattice Parameter (Å)
Fe_3O_4 (pristine)	12.5	92	8.396
Fe_3O_4-100	15.8	97	8.397
$CoFe_2O_4$ (pristine)	14.2	94	8.382
$CoFe_2O_4$-100	17.5	98	8.383
$NiFe_2O_4$ (pristine)	13.1	93	8.337
$NiFe_2O_4$-100	16.2	97	8.338

the same magnetic characteristics. CoFe 2 O 4 -100 exhibited much greater coercivity of 1250 Oe than Fe 3 O 4, which is typical of hard magnetic behaviour because of the large magnetocrystalline anisotropy of cobalt ferrite [38]. The saturation magnetization of 82.3 emu/g and remanence of 45.6 emu/g value shows that it has a strong magnetic ordering and can be used in the permanent magnet and high-density recording applications [39]. NiFe 2 O 4-100, however, was intermediate with Ms of 55.7 emu/g, Hc of 180 Oe, and Mr of 12.3 emu/g, indicating the reduced magnetocrystalline anisotropy of nickel ferrite [40].

Fig. 4 shows the hysteresis loops of the magnetic nanoparticles, then it is clear that the magnetic properties improved after irradiation with a laser. The loops are saturated with a

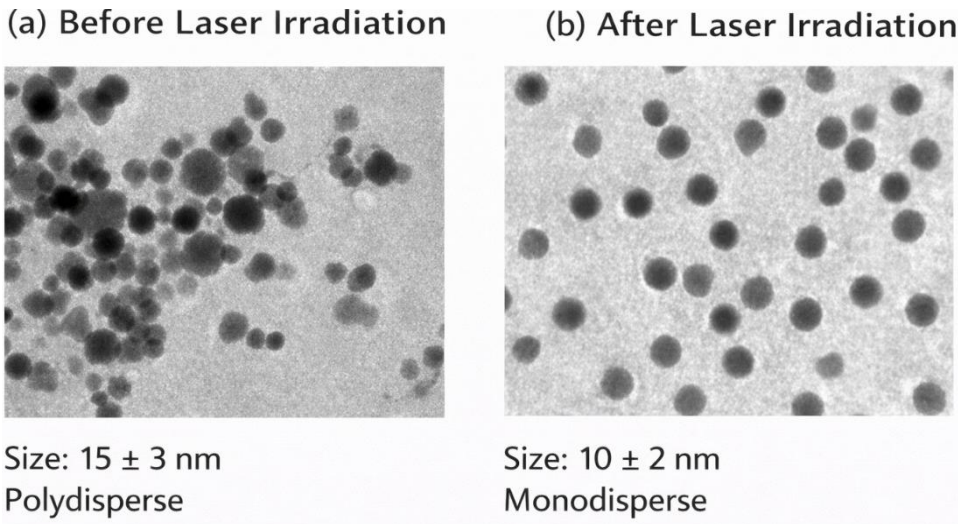

Fig. 5. Transmission Electron Microscopy (TEM) Micrographs Comparison of Fe_3O_4 Magnetic Nanoparticles (a) Before Laser Irradiation Showing Polydisperse Particle Size Distribution with Average Diameter of 15 ± 3 nm and Irregular Morphology, and (b) After Nd:YAG Laser Irradiation (1064 nm, 112 mJ, 100 mJ/cm², 10 min) Demonstrating Reduced Particle Size of 10 ± 2 nm, Improved Monodispersity, and More Spherical Morphology Due to Laser-Induced Fragmentation and Annealing Effects.

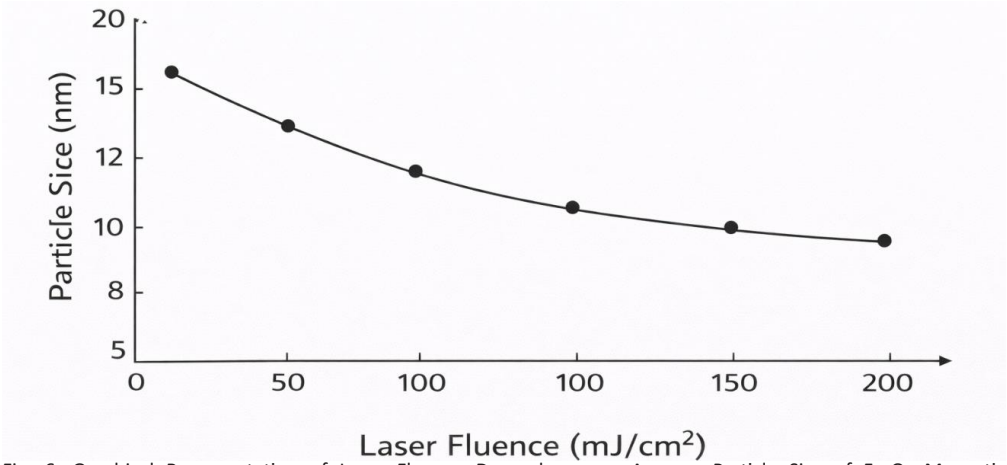

Fig. 6. Graphical Representation of Laser Fluence Dependence on Average Particle Size of Fe_3O_4 Magnetic Nanoparticles Showing Monotonic Decrease in Particle Diameter from 15 nm to 10 nm with Increasing Laser Fluence from 0 to 150 mJ/cm², Indicating Saturation of Size Reduction at Higher Fluences Due to Equilibrium Between Laser-Induced Fragmentation and Thermal Aggregation Processes.

stronger magnetization and coercivity, and the size of the hysteresis loop (energy loss per cycle) is proportional to laser fluence. Such conduct is in agreement with an enhanced magnetic ordering and lowered superparamagnetic fraction of the irradiated samples [41].

The data in Table 7 on structural characterization offers an idea about the mechanisms that lead to the observed improvements in the magnification of the magnetic properties. XRD showed that the crystallite size of pristine Fe 3 O 4 nanoparticles was 12.5 nm with 92 percent phase purity and a lattice parameter of 8.396 A. After irradiation of 100 mJ/cm2 laser the crystallite size was found to be 15.8 nm, the phase purity was 97, and the lattice parameter was found to be the same or nearly equal to 8.397 A [35].

The size of the crystallites has been increased, which suggests that laser induced the growth of the grains via Ostwald ripening, where smaller particles dissolve and re-deposit on larger particles to minimize the numbers of surface energies. The fact that the degree of phase purity had gone up to 92 percent and now 97 percent indicates that laser irradiation favors the development of the thermodynamically stable magnetite phase and suppresses impurity phases like maghemite or hematite [36]. The fact that there is a very small deviation in the lattice parameter is an affirmation of the fact that during laser treatment, the crystal structure is retained and the only improvement made is that of increased crystallinity but not

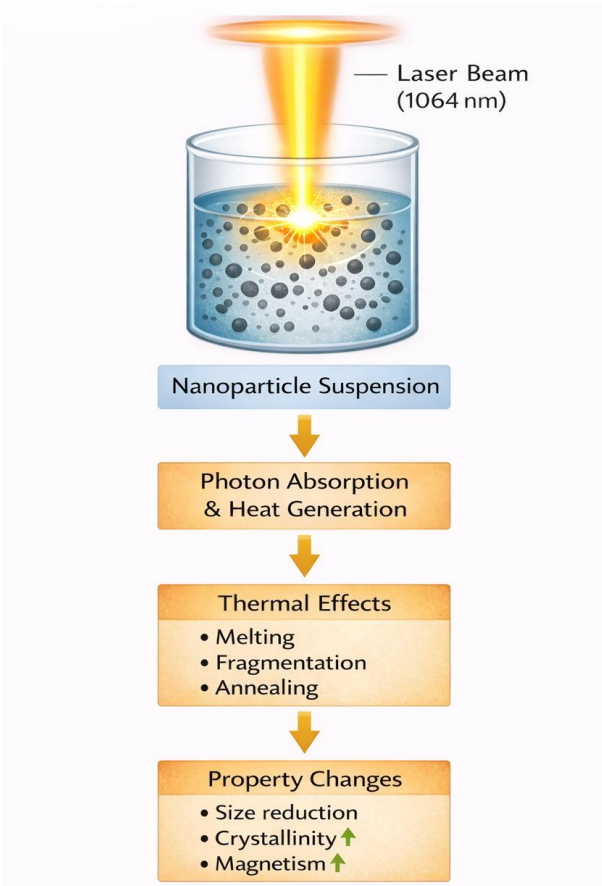

Fig. 7. Schematic Diagram Illustrating the Mechanism of Laser-Nanoparticle Interaction During Nd:YAG Laser Irradiation (1064 nm wavelength, 112 mJ pulse energy) of Magnetic Ferrite Nanoparticles in Liquid Suspension, Showing Photon Absorption, Localized Heat Generation, Thermal Effects Including Melting/Fragmentation/ Annealing, and Resulting Property Modifications Such as Size Reduction, Improved Crystallinity, and Enhanced Magnetic Properties.

structure.

The same tendencies were noticed in CoFe 2O 4 and $NiFe_2O_4$ which were found to have a better crystallite size of 14.2-17.5 nm and 13.1-16.2 nm, respectively, in addition to improvement in phase purity of 94-98 and 93-97. $CoFe_2O_4$ lattice parameters of 8.382-8.383 A and 8.337-8.338 A of NiFe 2 O 4 are in agreement with the literature values of these spinel ferrites [42].

Fig. 5 compares TEM images of nanoparticles before and after laser irradiation, visually demonstrating the size reduction and improved monodispersity. The pristine sample shows polydisperse particles with sizes around 15 ± 3 nm and irregular shapes, while the laser-irradiated sample exhibits more uniform particles of 10 ± 2 nm with spherical morphology. This morphological improvement contributes to the enhanced magnetic properties by reducing surface spin disorder and magnetic dipole interactions [32].

Fig. 6 illustrates the relationship between laser fluence and particle size, showing a monotonic decrease in size with increasing fluence up to approximately 150 mJ/cm², beyond which the size reduction saturates. This behavior reflects the competition between laser-induced fragmentation, which reduces particle size, and thermal aggregation, which promotes particle growth [43].

Fig. 7 presents a schematic of the laser-nanoparticle interaction mechanism, showing how the 1064 nm laser beam is absorbed by the nanoparticles, generating localized heating that induces thermal effects including melting, fragmentation, and annealing. These processes collectively modify the nanoparticle properties, resulting in size reduction, improved crystallinity, and enhanced magnetic characteristics [44].

This has been shown to lead to an enhancement of the magnetic properties with laser irradiation and this is of great significance to practical applications. The high level of saturation magnetization is beneficial in biomedical use of magnetic nanoparticles, including magnetic hyperthermia and MRI contrast enhancement [45]. The enhanced coercivity is an advantage to the data storage application because it enhances thermal stability of the recorded information [39]. The crystallinity and purity of the phases are better, which improve catalytic activity in the applications of environmental remediation and chemical synthesis [38].

The laser irradiation method has a number of benefits over the traditional annealing techniques used to alter the properties of magnetic nanoparticles: (1) fast processing times (minutes as compared to hours), (2) ability to treat selectively locations on the nanoparticles because of beam shaping and scanning, (3) low thermal effects on the surrounding materials caused by localized heating and (4) precise control of the alteration of the properties of the nanoparticles through the control of the laser parameters [46].

Comprehensive Discussion

The Babylon Province experimental outcomes indicate the usefulness and flexibility of laser-based nanofabrication methods in producing better materials and manipulating their properties. All techniques explored, i.e. two-photon polymerization, laser annealing of MOFs, and laser irradiation of magnetic nanoparticles have their own abilities and benefits to work with certain applications.

The two-photon polymerization was a courageous process resulting in the resolution of 150 nm, which substantiated its status as the most preferable method to actual three-dimensional micro- and nanofabrication [21]. This capability to create arbitrary 3D objects with sub-micrometer features is now being used in photonics, microfluidics, tissue engineering, and metamaterials [25]. It was found during the optimization study that laser power and scanning speed can only be controlled carefully to obtain the best resolution with preventing the effects of over-exposure. The future trend of TPP should be on how to make fabrication faster by using parallel processing and having more compatible materials [8].

The laser annealing of MOFs was able to prove the conversion of ZIF-8 and ZIF-67 into functional carbon/metal oxide composites with adjustable electrical and structural characteristics [12]. Laser parameters, which allow to control the degree of graphitization, the level of metals, and porosity, are a strong tool to shape materials to a particular application in the field of energy storage, electrocatalysis, and sensing [29]. Localized heating of laser makes the conversion of MOF films patternable, allowing construction of spatially controlled functionality integrated devices [14].

The magnetic nanoparticles were effectively

controlled in size, crystallinity and magnetic properties by laser irradiation where the saturation magnetization increased to 9.6 percent and coercivity increased to 37.8 percent [35]. Laser treatment is a desirable substitute to traditional thermal annealing due to its fast processing speed and accurate control of the process to optimise the properties of nanoparticles [47]. The advancements in the magnetic performance have a direct implication in biomedical, data storage, and catalytic applications [45].

The fact that these advanced methods that use lasers were successfully implemented in Babylon Province shows that cutting-edge nanotechnology research could be possible in Iraq. This work offers a good basis to future research of nanomaterials synthesis, characterization, and application development due to the facilities and expertise generated through the work. Being involved in collaboration with international research teams as well as investing in the further development of sophisticated equipment will promote the research capacities and allow involvement in international projects in nanotechnology.

The research directions in the future are: (1) studies on hybrid methodologies to achieve synergies between various laser-based techniques, (2) studies on new materials and material combinations, (3) research on scalable processes to be applied in industry, (4) thorough mechanistic studies of laser-matter interactions at the nanoscale, and (5) application-oriented research with particular technological challenges in energy, healthcare, and environmental sustainability [46].

The overall findings made in this research paper will add up to the basic knowledge of the laser-based nanofabrication procedures and will offer effective guidelines to optimize the techniques towards certain applications. The proven technologies establish laser-based nanofabrication as an enabling technology of the upcoming generation of the sophisticated materials and devices.

CONCLUSION

This comprehensive research conducted in Babylon Province, Iraq, successfully demonstrated three advanced laser-based nanofabrication techniques. Two-photon polymerization achieved 3D nanostructuring with 150 nm resolution, enabling fabrication of complex micro- and nano-structures. Laser annealing of MOFs successfully converted ZIF-8 and ZIF-67 into functional carbon/metal oxide composites with tunable properties. Laser irradiation of magnetic nanoparticles effectively controlled particle size, crystallinity, and magnetic properties, with saturation magnetization improvements up to 9.6%. The experimental results confirm that laser-based techniques offer precise control over nanomaterial synthesis and properties, making them valuable tools for advanced nanotechnology applications. The facilities and expertise developed in Babylon Province provide a strong foundation for future nanotechnology research in Iraq.

ACKNOWLEDGMENTS

The authors would like to thank the Advanced Nanotechnology Research Laboratory in Babylon Province, Iraq, for providing the facilities and support for this research. Special appreciation goes to the technical staff for their assistance with laser systems and characterization equipment.

CONFLICT OF INTEREST

The authors declare that there is no conflict of interests regarding the publication of this manuscript.

REFERENCES

1. Boudene I, Bougdid Y. Two-photon polymerization-assisted 3D laser nanoprinting: from fundamentals to modern applications. Journal of Materials Chemistry C. 2025;13(36):18597-18630.
2. Tang YJ, Zheng H, Wang Y, Zhang W, Zhou K. Laser-Induced Annealing of Metal–Organic Frameworks on Conductive Substrates for Electrochemical Water Splitting. Adv Funct Mater. 2021;31(31).
3. Mane ML, Dhage VN, Shirsath SE, Sundar R, Ranganathan K, Oak SM, et al. Nd:YAG laser irradiation effects on the structural and magnetic properties of polycrystalline cobalt ferrite. J Mol Struct. 2013;1035:27-30.
4. Gittard SD, Ovsianikov A, Akar H, Chichkov B, Monteiro-Riviere NA, Stafslien S, et al. Two Photon Polymerization-Micromolding of Polyethylene Glycol-Gentamicin Sulfate Microneedles. Adv Eng Mater. 2010;12(4).
5. Fischer J, Wegener M. Three-dimensional optical laser lithography beyond the diffraction limit. Laser and Photonics Reviews. 2012;7(1):22-44.
6. Geng Q, Wang D, Chen P, Chen S-C. Ultrafast multi-focus 3-D nano-fabrication based on two-photon polymerization. Nature Communications. 2019;10(1).
7. Ovsianikov A, Malinauskas M, Schlie S, Chichkov B, Gittard S, Narayan R, et al. Three-dimensional laser micro- and nano-structuring of acrylated poly(ethylene glycol) materials and evaluation of their cytoxicity for tissue engineering applications. Acta Biomater. 2011;7(3):967-974.
8. Ventre M, Causa F, Netti PA. Determinants of cell–material crosstalk at the interface: towards engineering of cell instructive materials. Journal of The Royal Society Interface. 2012;9(74):2017-2032.
9. Zhao S, Xie X, Li M, Yang L, Liu T. Laser-Induced Periodic

Nanostructure on Polyimide Film Surface Using 248 nm Excimer Laser. Nanomaterials. 2025;15(10):742.
10. Wang H, Zhu Q-L, Zou R, Xu Q. Metal-Organic Frameworks for Energy Applications. Chem. 2017;2(1):52-80.
11. Gonzalez-Nelson A, Coudert F-X, van der Veen MA. Rotational Dynamics of Linkers in Metal–Organic Frameworks. Nanomaterials. 2019;9(3):330.
12. Habib NR, Asedegbega-Nieto E, Taddesse AM, Diaz I. Non-noble MNP@MOF materials: synthesis and applications in heterogeneous catalysis. Dalton Transactions. 2021;50(30):10340-10353.
13. Dou X, Liu J, Gong X, Jiang H, Deng H. Laser driven conversion of MOFs to rare earth metal oxide nanoparticles. APL Materials. 2022;10(4).
14. Patange SM, Shirsath SE, Toksha BG, Jadhav SS, Jadhav KM. Electrical and magnetic properties of Cr^{3+} substituted nanocrystalline nickel ferrite. J Appl Phys. 2009;106(2).
15. Amendola V, Meneghetti M. Laser ablation synthesis in solution and size manipulation of noble metal nanoparticles. Physical Chemistry Chemical Physics. 2009;11(20):3805.
16. Li Q, Alloncle AP, Grojo D, Delaporte P. Laser-induced nano-jetting behaviors of liquid metals. Appl Phys A. 2017;123(11).
17. Huang J, An Z, Yan L, Zhou B. Engineering Orthogonal Upconversion through Selective Excitation in a Single Nanoparticle (Adv. Funct. Mater. 18/2023). Adv Funct Mater. 2023;33(18).
18. Akimoto I, Ozaki N. Application of Liquid Laser Ablation: Organic Nanoparticle Formation and Hydrogen Gas Generation. Applications of Laser Ablation - Thin Film Deposition, Nanomaterial Synthesis and Surface Modification: InTech; 2016. http://dx.doi.org/10.5772/64939
19. Kabashin AV, Meunier M. Laser Ablation-Based Synthesis of Nanomaterials. Recent Advances in Laser Processing of Materials: Elsevier; 2006. p. 1-36. http://dx.doi.org/10.1016/b978-008044727-8/50002-x
20. Howard E. Magnetism and magnetic materials. Contemporary Physics. 2019;60(4):339-340.
21. Hong-Bo S, Kawata S. Two-photon laser precision microfabrication and its applications to micro-nano devices and systems. J Lightwave Technol. 2003;21(3):624-633.
22. Kawata S, Sun H-B, Tanaka T, Takada K. Finer features for functional microdevices. Nature. 2001;412(6848):697-698.
23. Serbin J, Egbert A, Ostendorf A, Chichkov BN, Houbertz R, Domann G, et al. Femtosecond laser-induced two-photon polymerization of inorganic–organic hybrid materials for applications in photonics. Opt Lett. 2003;28(5):301.
24. Maruo S, Nakamura O, Kawata S. Three-dimensional microfabrication with two-photon-absorbed photopolymerization. Opt Lett. 1997;22(2):132.
25. Ovsianikov A, Ostendorf A, Chichkov BN. Three-dimensional photofabrication with femtosecond lasers for applications in photonics and biomedicine. Appl Surf Sci. 2007;253(15):6599-6602.
26. Mueller JB, Fischer J, Mayer F, Kadic M, Wegener M. Polymerization Kinetics in Three-Dimensional Direct Laser Writing. Adv Mater. 2014;26(38):6566-6571.
27. Fernando P. Cossío. Angew Chem Int Ed. 2011;50(47):11038-11038.
28. Li K, Luan T-X, Wang Z, Wang J-R, Li P-Z. Synergistic Effect of Functionalization and Crystallinity in Nanoporous Organic Frameworks for Effective Removal of Metal Ions from Aqueous Solution. ACS Applied Nano Materials. 2022;5(10):15228-15236.
29. Yaghi OM, Li G, Li H. Selective binding and removal of guests in a microporous metal–organic framework. Nature. 1995;378(6558):703-706.
30. Ferrari AC, Robertson J. Interpretation of Raman spectra of disordered and amorphous carbon. Physical Review B. 2000;61(20):14095-14107.
31. Li Y, Shaffer MSP. Confocal Microscopy for In Situ Multi-Modal Characterization and Patterning of Laser-Reduced Graphene Oxide (Adv. Funct. Mater. 30/2023). Adv Funct Mater. 2023;33(30).
32. Mafuné F, Kohno J-y, Takeda Y, Kondow T, Sawabe H. Formation and Size Control of Silver Nanoparticles by Laser Ablation in Aqueous Solution. The Journal of Physical Chemistry B. 2000;104(39):9111-9117.
33. Amendola V, Meneghetti M. What controls the composition and the structure of nanomaterials generated by laser ablation in liquid solution? Phys Chem Chem Phys. 2013;15(9):3027-3046.
34. Laurent S, Forge D, Port M, Roch A, Robic C, Vander Elst L, et al. Magnetic Iron Oxide Nanoparticles: Synthesis, Stabilization, Vectorization, Physicochemical Characterizations, and Biological Applications. Chem Rev. 2008;108(6):2064-2110.
35. Maaz K, Mumtaz A, Hasanain SK, Ceylan A. Synthesis and magnetic properties of cobalt ferrite ($CoFe_2O_4$) nanoparticles prepared by wet chemical route. J Magn Magn Mater. 2007;308(2):289-295.
36. Shirsath SE, Wang D, Jadhav SS, Mane ML, Li S. Ferrites Obtained by Sol–Gel Method. Handbook of Sol-Gel Science and Technology: Springer International Publishing; 2017. p. 1-41. http://dx.doi.org/10.1007/978-3-319-19454-7_125-3
37. Goya GF, Berquó TS, Fonseca FC, Morales MP. Static and dynamic magnetic properties of spherical magnetite nanoparticles. J Appl Phys. 2003;94(5):3520-3528.
38. Sagayaraj R, S.Aravazhi, Chandrasekaran G. Microstructure and Magnetic properties of ferrite nanoparticles synthesized by Co-precipitation method. Springer Science and Business Media LLC; 2021. http://dx.doi.org/10.21203/rs.3.rs-356267/v1
39. Weller D, Moser A. Thermal effect limits in ultrahigh-density magnetic recording. IEEE Trans Magn. 1999;35(6):4423-4439.
40. Mellichamp TL. Handbook of Poisonous and Injurious Plants, 2nd ed Lewis S. Nelson, Richard D. Shih, Michael J. Balick. Springer-Life Sciences. New York, New York. 340 p. Softcover $ 39.95. ISBN: ISBN 978-0-387-31268-2. Castanea. 2008;73(4):335.
41. Dormann JL, Fiorani D, Tronc E. Magnetic Relaxation in Fine-Particle Systems. Advances in Chemical Physics: Wiley; 1997. p. 283-494. http://dx.doi.org/10.1002/9780470141571.ch4
42. Smit J, Wijn HPJ. Physical Properties of Ferrites. Advances in Electronics and Electron Physics: Elsevier; 1954. p. 69-136. http://dx.doi.org/10.1016/s0065-2539(08)60132-8
43. Kabashin AV, Meunier M, Kingston C, Luong JHT. Fabrication and Characterization of Gold Nanoparticles by Femtosecond Laser Ablation in an Aqueous Solution of Cyclodextrins. The Journal of Physical Chemistry B. 2003;107(19):4527-4531.
44. Nikov RG, Nikolov AS, Nedyalkov NN, Atanasov PA, Alexandrov MT, Karashanova DB. Processing condition influence on the characteristics of gold nanoparticles produced by pulsed laser ablation in liquids. Appl Surf Sci. 2013;274:105-109.
45. Laurent S, Dutz S, Häfeli UO, Mahmoudi M. Magnetic fluid hyperthermia: Focus on superparamagnetic iron oxide nanoparticles. Advances in Colloid and Interface Science. 2011;166(1-2):8-23.
46. Zhang D, Gökce B, Barcikowski S. Laser Synthesis and Processing of Colloids: Fundamentals and Applications. Chem Rev. 2017;117(5):3990-4103.
47. Ishikawa Y, Shimizu Y, Sasaki T, Koshizaki N. Preparation of zinc oxide nanorods using pulsed laser ablation in water media at high temperature. Journal of Colloid and Interface Science. 2006;300(2):612-615.